Theoretical insight into complexation between cyclocarbons and C_{60} fullerene

Zeyu Liu[a] and Tian Lu[b,*]

[a] School of Environmental and Chemical Engineering, Jiangsu University of Science and Technology, Zhenjiang 212100, People's Republic of China

[b] Beijing Kein Research Center for Natural Sciences, Beijing 100022, People's Republic of China (www.keinsci.com)

Abstract: This work conducts the comprehensive theoretical study on the non-covalent complexation between cyclocarbons of different sizes and C_{60} fullerene for the first time. The binding energy between cyclocarbons and C_{60} fullerene is observed to be significantly stronger than that between two C_{18} or two C_{60} fullerenes, indicating a particularly strong affinity between them. The cyclocarbons and C_{60} fullerene can spontaneously assemble into non-covalent complexes characterized by π-π stacking in the gas phase at room temperature, and the hydrophobic effect caused by the solvent environment can promote this binding. From C_{18} to C_{34}, the binding strength with C_{60} fullerene increases almost linearly with the increase of cyclocarbon size, and the C_{34}@C_{60} dimer exhibits a perfect nano-Saturn structure. By studying the trimers of 2:1 form between cyclocarbons and C_{60} fullerene, it is observed that as the ring size increases, the angle between the two cyclocarbons gradually decreases. In the largest trimer we studied, C_{60}@2C_{34}, the fullerene is symmetrically surrounded by two cyclocarbons. The results on the trimers formed by cyclocarbon and C_{60} fullerenes in a 1:2 ratio showed when the size of the cyclocarbon sandwiched between two fullerenes is not quite large, the trimers exhibit an ideal dumbbell-like structure, and the presence of the first fullerene has a significant synergistic effect on the binding of the second one. Combined with the analysis of interaction energy and van der Waals potential, we

https://doi.org/10.26434/chemrxiv-2024-hs2sz **ORCID:** https://orcid.org/0000-0002-7079-1907 Content not peer-reviewed by ChemRxiv. **License:** CC BY 4.0

found that the cyclocarbon greatly promotes the non-covalent dimerization of fullerenes, which acted as a “molecular glue”.

Table of Contents:

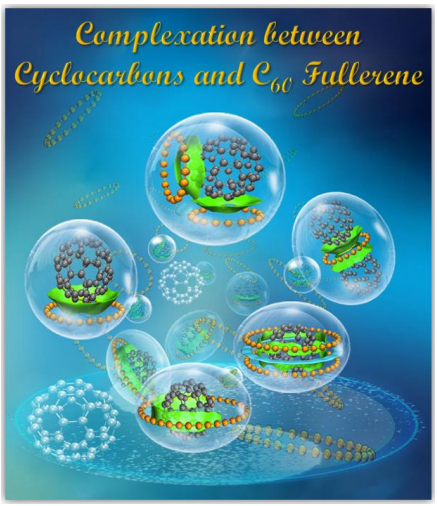

Keywords: cyclocarbon, fullerene, non-covalent interaction, π-π stacking, binding energy, interaction energy

https://doi.org/10.26434/chemrxiv-2024-hs2sz **ORCID:** https://orcid.org/0000-0002-7079-1907 Content not peer-reviewed by ChemRxiv. **License:** CC BY 4.0

1. Introduction

Cyclocarbon is a cyclic molecule composed of *sp*-hybridized carbons connected to each other. Earlier, cyclocarbons have been explored experimentally and there are evidences of their formation in the gas phase,[1-4] but for a long time, no one can provide direct molecular morphology for them. In 2019, cyclo[18]carbon (C_{18}) was first observed in the condensed phase,[5] ending a long-standing controversy over the structure of this unique carbon allotrope and reigniting a wave of research on it. Over the next three years, scientists synthesized cyclo[*n*]carbon molecules with various sizes, including n = 6,[6] 10,[7] 12,[6] 13,[8] 14,[7] 16,[9] 20,[10] and 26.[8] Theoretical chemists have also conducted extensive research on the special properties and potential applications of cyclocarbon systems in recent years, among which we have achieved meaningful results in many aspects of C_{18} and related compounds, including geometric structure, electronic structure, ring strain, aromaticity, optical nonlinearity, intermolecular interaction, external field effect, dynamic behavior, excited state, and so on.[11-27]

Multiple works have speculated or confirmed that the high reactivity of cyclocarbons and their precursors allows them to fuse through covalent coupling, opening up avenues for molecular polymerization into bigger carbon rings.[5,9] There are also indications that cyclocarbons are valuable precursors for building three-dimensional carbon networks[28] and forming fullerenes in graphite vapor.[29] These statements all imply the possibility of encountering cyclocarbon molecules and other carbon materials in real space. Graphene and C_{60} fullerene are recognized as two of the most typical carbon materials, which have had a great impact on the development of chemistry and materials.[30,31] Recently, Chen et al. performed the interaction of C_{18} with graphene by periodic and non-periodic calculations.[32] The nature of the interaction between C_{18} and graphene was found to be essentially the same as that between monomers in C_{18} dimer, but all components of the high order symmetry-adapted perturbation theory (SAPT) in C_{18}-graphene complex are about three times as large as those in C_{18} dimer, indicating that the intermolecular interaction

https://doi.org/10.26434/chemrxiv-2024-hs2sz **ORCID:** https://orcid.org/0000-0002-7079-1907 Content not peer-reviewed by ChemRxiv. **License:** CC BY 4.0

is much stronger in the former. This conclusion is strictly consistent with our results obtained by high-precision quantum chemical calculations[20,24]. As of now, however, the complexation behavior of cyclocarbons with C_{60} fullerene has not been reported. The circular cavity of cyclocarbons and spherical structure of C_{60} fullerene inevitably lead to novel interactions between them, which is worth exploring in depth. Whether cyclocarbons can stably bind with C_{60} fullerene and what the form of the resulting complex are not only very interesting theoretical questions, but also of great significance for the future design and utilization of their composite systems.

In this study, we performed a comprehensive quantum chemical study of the complexation between cyclocarbons and C_{60} fullerenes. The cyclo[*n*]carbons with an even number of carbons from n = 18 to 36 (C_n, n = 18, 20, 22, 24, 26, 28, 30, 32, 34, and 36) are considered. We not only examine dimers formed between cyclocarbons and C_{60} fullerene ($C_{60}@C_n$), but also consider trimers composed of them in 1:2 and 2:1 manners ($C_{60}@2C_n$ and $2C_{60}@C_n$, respectively). The geometric structure, binding strength, and interaction nature of the complexes are explored in detail.

2. Computational Details

Our previous studies have shown that a density functional theory (DFT) method with a high amount of Hartree-Fock (HF) exchange (usually more than 25%) are necessary to correctly describe the ground-state geometry of C_{18}, and that ωB97XD[33] functional with 6-311G(d)[34] basis set can give acceptable results[15,19,24,27]. So, in this work, all systems studied were optimized at the ωB97XD/6-311G(d) level, and frequency analyses were subsequently calculated. The Gaussian 16 program[35] is used in these stages. All optimized structures in *xyz* format are given in the Supplemental Information (SI). In order to obtain as accurate binding energies as possible, for the studied $C_{60}@C_n$ dimers, the involved single point energies were evaluated using the very accurate ωB97M-V[36]/def2-QZVPP[37] level by ORCA 5.0.4 program.[38] The ωB97M-V functional shows superior performance in evaluating intermolecular interaction energies,[36] and its 100% HF exchange at long range enables it to

https://doi.org/10.26434/chemrxiv-2024-hs2sz **ORCID:** https://orcid.org/0000-0002-7079-1907 Content not peer-reviewed by ChemRxiv. **License:** CC BY 4.0

represent cyclocarbon reasonably like the ωB97XD. The def2-QZVPP is a fairly large basis set and essentially free of basis set superposition error (BSSE),[39] thus it is well-suited for estimating intermolecular binding energies. However, the def2-QZVPP basis set is too expensive to study trimers in this work, which contains up to 150 carbon atoms, so the single point energies used to derive binding energies for all them were calculated using cheaper def2-TZVP[37] instead, and geometrical counterpoise (gCP) method[40] was employed to empirically correct for nonnegligible BSSE.

The thermal corrections to free energies of gas-phase standard state (298.15 K, 1 atm) were derived by Shermo 2.5 code[41] through Grimme's quasi-rigid-rotor harmonic oscillator model.[42] Scanning of free energy at different temperatures was also realized via Shermo. Free energies in the aqueous phase at solution standard state (298.15 K, 1 M) were calculated as sum of free energies in the gas phase and solvation free energies (ΔG_{soln}), the latter were obtained via solvation model based on density (SMD)[43] in combination with the M05-2X/6-31G(d) level, which was found to be the most ideal strategy to estimate ΔG_{soln}.[43] 1.89 kcal/mol has been included into ΔG_{soln} to account for concentration change from gas to solution standard states.[44]

The sobEDAw energy decomposition analysis[45] was conducted by Multiwfn 3.8(dev) code[46] in combination with Gaussian 16 program. Independent gradient model based on Hirshfeld partition (IGMH),[47,48] Mayer bond order, fragment charge calculations, and evaluation of van der Waals (vdW) potential were all realized by Multiwfn 3.8(dev) code based on the ωB97XD/6-311G(d) wavefunction at optimized structures. All isosurfaces and molecular structure maps were rendered by VMD 1.9.3 program,[49] and colored section maps were plotted by VESTA 3.5.8.[50]

3. Results and Discussion

3.1 Dimerization between cyclocarbons and C_{60} fullerene

We first studied the dimers composed of a C_n (n = 18, 20, 22, 24, 26, 30, 32, 34, and 36) and a C_{60} fullerene, $C_{60}@C_n$. Two minimum structures of $C_{60}@C_{18}$ were located, as shown in Fig. S1, in which the C_{18} faces the hexagonal and pentagonal

https://doi.org/10.26434/chemrxiv-2024-hs2sz **ORCID:** https://orcid.org/0000-0002-7079-1907 Content not peer-reviewed by ChemRxiv. **License:** CC BY 4.0

rings of C_{60} fullerene, respectively. The former is 0.9 kcal/mol lower in energy than the latter, so in subsequent research, we will only focus on the configuration of the former.

Five representative $C_{60}@C_n$ dimers are presented in Fig. 1. It can be seen that as the size of the cyclocarbon increases, C_{60} fullerene gradually submerges into the carbon ring. When the cyclocarbon reaches C_{34}, since the interior region of the ring is large enough to completely accommodate the C_{60} fullerene, the centers of the two moieties coincide exactly, forming a $C_{34}@C_{60}$ structure that is a new example of nano-Saturn.[51] As the cyclocarbon expands further to C_{36}, the center of the C_{60} fullerene spontaneously deviates from the center of the carbon ring to maximize their intermolecular attraction.

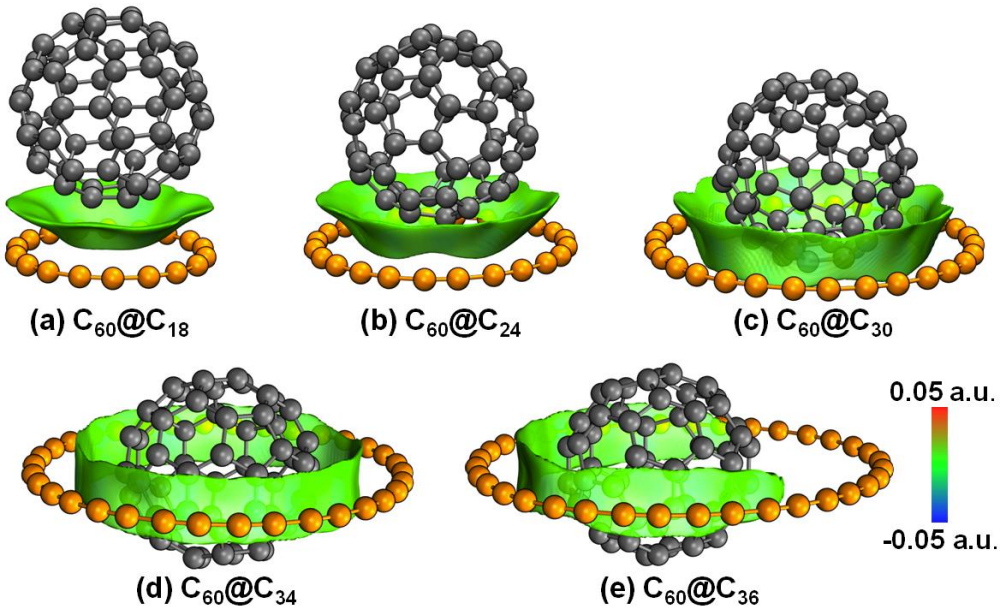

Fig. 1 Optimized geometry of $C_{60}@C_n$ dimers (n = 18, 24, 30, 34, and 36). Isosurfaces of δg^{inter} function with isovalue of 0.002 a.u. colored by $sign(\lambda_2)\rho$ according to the color bar are also shown.

IGMH is a popular method for visualizing interactions in chemical systems.[47,48] The δg^{inter} function defined in the framework of IGMH is able to clearly reveal the interaction between specific fragments in terms of isosurfaces. If the isosurfaces are

https://doi.org/10.26434/chemrxiv-2024-hs2sz **ORCID:** https://orcid.org/0000-0002-7079-1907 Content not peer-reviewed by ChemRxiv. **License:** CC BY 4.0

colored by $sign(\lambda_2)\rho$, the interaction type can also be easily distinguished. The $sign(\lambda_2)\rho$ colored δg^{inter} isosurfaces for $C_{60}@C_n$ are also shown in Fig. 1, where cyclocarbon and C_{60} fullerene are defined as the two fragments used for analysis. The δg^{inter} isosurfaces intuitively display the regions where significant intermolecular interactions occur, and the completely green color indicates that the electron density in the regions is very low, which corresponds to the typical feature of dispersion-dominated interactions. Considering that both cyclocarbons and C_{60} fullerene have rich π electrons and the nature of π-π stacking arises precisely from the dispersion effect between parallel distributed π electrons, and moreover, that the very flat shape of δg^{inter} isosurfaces between π-conjugated fragments in Fig. 1 is a typical signal of π-π stacking,[15,24,47,48] the complexation between cyclocarbons and C_{60} fullerene can be unambiguously regarded as driving by the π-π stacking effect.

To quantitatively compare the binding strength between various cyclocarbons and C_{60} fullerene, we calculated binding energies based on electronic energies (ΔE_{bind}) as well as binding free energies of gas-phase ($\Delta G°_{bind}(gas)$) and aqueous-phase ($\Delta G°_{bind}(aq)$) at respective standard states. ΔE_{bind} was calculated using standard definition, that is $\Delta E_{bind} = E(C_{60}@C_n) - [E(C_{60}) + E(C_n)]$, where E represents electronic energy evaluated at the respective optimized geometry. $\Delta G°_{bind}(gas)$ and $\Delta G°_{bind}(aq)$ were calculated by a similar way, but using free energies in the corresponding phases instead. The results of binding energies are collectively plotted in Fig. 2, and the raw data are given in Table S1.

https://doi.org/10.26434/chemrxiv-2024-hs2sz **ORCID:** https://orcid.org/0000-0002-7079-1907 Content not peer-reviewed by ChemRxiv. **License:** CC BY 4.0

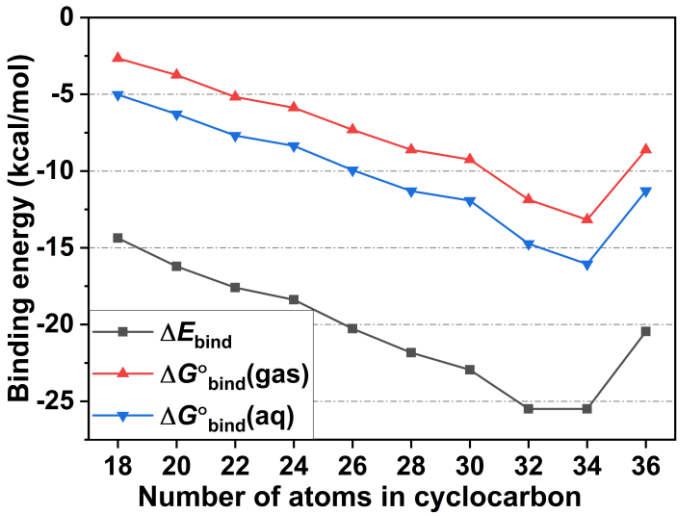

Fig. 2 Binding electronic energies (ΔE_{bind}) as well as binding free energies in gas-phase standard state and in aqueous-phase standard state ($\Delta G°_{bind}$(gas) and $\Delta G°_{bind}$(aq), respectively) of C_n@C_{60} dimers.

It can be seen that the binding strength steadily increases with increasing the size of cyclocarbon until C_{34}. This can be easily understood from the variation of δg^{inter} isosurfaces in Fig. 1, namely, the larger the cyclocarbon, the wider its prominent interaction region with C_{60} fullerene. The areas of the isosurfaces have a very good linear relationship with the binding energies (R^2 = 0.973) as shown in Fig. S2, indicating that the isosurface area is a useful descriptor for predicting the strength of π-π interactions without conducting energy calculations. It is found that C_{36} interacts less strongly with C_{60} fullerene than C_{34}, mainly because the ring size of C_{36} is too large for fullerene to interact tightly with all its atoms simultaneously, as clearly illustrated by the IGMH map in Fig. 1(e).

Due to the large reduction of entropy caused by the complexation of cyclocarbons and C_{60} fullerene, the entropy penalty effect makes $\Delta G°_{bind}$(gas) much more positive than ΔE_{bind}. However, since all $\Delta G°_{bind}$(gas) data in Fig. 2 are still evidently negative, the formation of C_{60}@C_n dimers must occur spontaneous in the gas phase, at least at room temperature. Furthermore, one can see that all $\Delta G°_{bind}$(aq) are systematically more negative than $\Delta G°_{bind}$(gas) by several kcal/mol, indicating that aqueous environment can facilitate the formation of the C_{60}@C_n dimers. As is well

https://doi.org/10.26434/chemrxiv-2024-hs2sz **ORCID:** https://orcid.org/0000-0002-7079-1907 Content not peer-reviewed by ChemRxiv. **License:** CC BY 4.0

known, the hydrophobic effect significantly promotes the aggregation of nonpolar substances in aqueous solution, thus this phenomenon also reflects the strong hydrophobic properties of the monomers.

Fig. 3 displays variation of $\Delta G°_{bind}$(gas) with respect to temperature for $C_{60}@C_{18}$, $C_{60}@C_{34}$, and $C_{60}@C_{36}$. It can be clearly seen that the higher the temperature, the more positive the $\Delta G°_{bind}$(gas) and the stronger the tendency for dissociation of the complexes, that is, the lower the possibility of forming complexes. The temperatures at which the $\Delta G°_{bind}$(gas) equal to 0 corresponds to the critical temperature (T^{crit}) for formation of the dimers in the gas phase, which are labelled in Fig. 3. The T^{crit} = 366 K of $C_{60}@C_{18}$ indicates that the dimer can remain stable to some extent above room temperature. As mentioned above, C_{34} has the strongest tendency of complexation with C_{60} fullerene compared with other cyclocarbons, and correspondingly, the T^{crit} of $C_{60}@C_{34}$ of 605 K corresponds to the highest temperature that a cyclocarbon can form a dimer with C_{60} fullerene. The T^{crit} of $C_{60}@C_{36}$ is calculated to be of 505 K, which is significantly lower than that of $C_{60}@C_{34}$, suggesting that cyclocarbons larger than C_{34} do not have a higher ability to bind C_{60} fullerene non-covalently from a thermodynamic point of view.

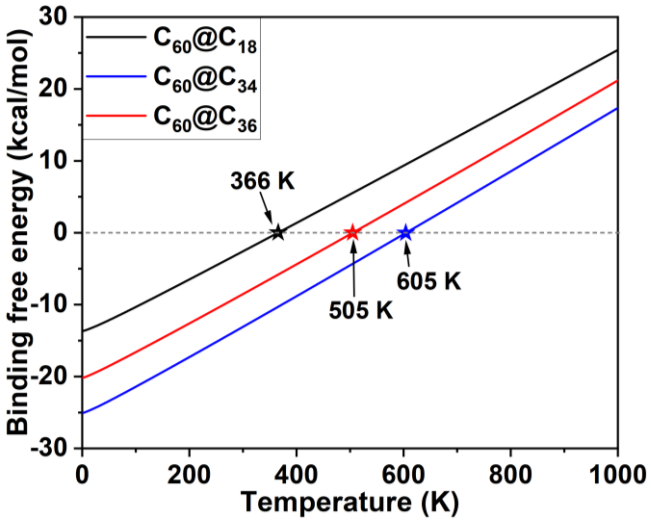

Fig. 3 Variation of binding free energy of $C_{60}@C_{18}$, $C_{60}@C_{34}$, and $C_{60}@C_{36}$ with respect to temperature in the gas phase of 1 atm pressure.

https://doi.org/10.26434/chemrxiv-2024-hs2sz **ORCID:** https://orcid.org/0000-0002-7079-1907 Content not peer-reviewed by ChemRxiv. **License:** CC BY 4.0

Due to the flexibility of cyclocarbons,[25] their complexation with C_{60} fullerene may lead to deformation in different degrees. To quantify this effect, we calculated the deformation energy (ΔE_{def}) of the cyclocarbons in different $C_{60}@C_n$ dimers, and the data are given in Table S1. It can be seen that the ΔE_{def} is almost zero from C_{18} to C_{34}, showing that the deformation of ring structures during complexation is negligible. However, the ΔE_{def} reaches 1.0 kcal/mol in the case of C_{36}, indicating that evident ring deformation due to the asymmetric interaction between C_{36} and C_{60} fullerene. The superposition map of C_{36} in isolated state and after complexation in Fig. S3 shows a notable elongation of the ring in the latter case.

It is worth mentioning that we have reported an interaction energy of -9.2 kcal/mol between the monomers in the π-π stacking dimer formed by two C_{18},[24] while the binding energy of $C_{60}@C_{18}$ obtained in this work is -14.4 kcal/mol. This indicates the interaction strength between C_{18} and C_{60} fullerene is significantly stronger than that between two C_{18}. In addition, the binding energy of $C_{60}@C_{18}$ is also significantly greater than that between two C_{60} fullerenes, estimated to be -8.3 kcal/mol by the very accurate DLPNO-CEPA/1 method with complete basis set extrapolation.[52] Therefore, we can conclude that the cyclocarbon systems have an inherent strong affinity with C_{60} fullerene.

In order to gain a deeper understanding of the interaction between cyclocarbons and C_{60} fullerenes, we performed energy decomposition analysis on the representative complex $C_{60}@C_{18}$ at the BHandHLYP-D3(BJ)[39,53]/6-311+G(2d,p)[34] level via the robust and universal sobEDAw method,[45] using complex basis functions to suppress BSSE in monomer calculations. The BHandHLYP functional has been shown to be able to reasonably characterize C_{18},[27] and is also satisfactory in assessing intermolecular interactions if used in combination with DFT-D3(BJ) dispersion correction.[54] The interaction energy between C_{18} and C_{60} fullerene at this level is -12.0 kcal/mol, which is close to the results by ωB97M-V/def2-QZVPP calculation (-14.4 kcal/mol). The contributions of different physical components to the interaction energy analyzed by sobEDAw are: -8.4 kcal/mol electrostatic, 25.6 kcal/mol

https://doi.org/10.26434/chemrxiv-2024-hs2sz **ORCID:** https://orcid.org/0000-0002-7079-1907 Content not peer-reviewed by ChemRxiv. **License:** CC BY 4.0

exchange-repulsion, -2.4 kcal/mol orbital, and -26.8 kcal/mol dispersion. Clearly, the dispersion effect plays a crucial role in the complexation between C_{18} and C_{60} fullerene, while the electrostatic effect, although not negligible, only plays an auxiliary role in the formation of the dimer. The orbital interaction can be basically ignored, as its percentage contribution to the attractive component is merely 6.4%. Regarding these situations of the C_{60}@C_{18} dimer, it fully conforms to the typical characteristics of π-π stacking.[55] The conclusion of the above IGMH analysis has therefore been confirmed from an energy perspective.

We then calculated fragment charge of C_{18} in the C_{60}@C_{18} dimer using the Mulliken[56,57] and atomic dipole moment corrected Hirshfeld charge (ADCH)[58] methods for examining the extent of charge transfer between C_{18} and C_{60} fullerene. The results are 0.015 and -0.027 e, respectively, which are fairly low values indicating that intermolecular charge transfer is completely negligible. Furthermore, the total Mayer bond order[59] for all atomic pairs between C_{18} and C_{60} fullerene was calculated to estimate effective number of shared electron pairs between the two molecules. The very small value of 0.041 reflects that the C_{60}···C_{18} interaction is undeniable non-covalent.

With the discovery of two minimum structures of C_{60}@C_{18} dimer in mind, the possibility of relative rotation between C_{60} fullerene and cyclocarbons is also worth exploring. At the same computational level as geometry optimization, we located the transition state between C_{60}@C_{18} dimers of different configurations, which has a unique imaginary frequency of 9.8*i* cm^{-1}. The corresponding normal coordinate of the transition state is plotted as Fig. 4, which clearly demonstrates the relative sliding tendency of C_{60} relative to the C_{18} and characterizes the interconversion between the two configurations. The forward and reverse potential barriers calculated at the ωB97M-V/def2-QZVPP level are extremely low of 0.90 and 0.04 kcal/mol, respectively, indicating that configuration conversion can occur very frequently. For complexes formed by C_{60} fullerene and other cyclocarbons, due to their π-π interaction characteristics similar to that of C_{60}@C_{18}, relative motion between the two

https://doi.org/10.26434/chemrxiv-2024-hs2sz **ORCID:** https://orcid.org/0000-0002-7079-1907 Content not peer-reviewed by ChemRxiv. **License:** CC BY 4.0

molecules must also be very easy.

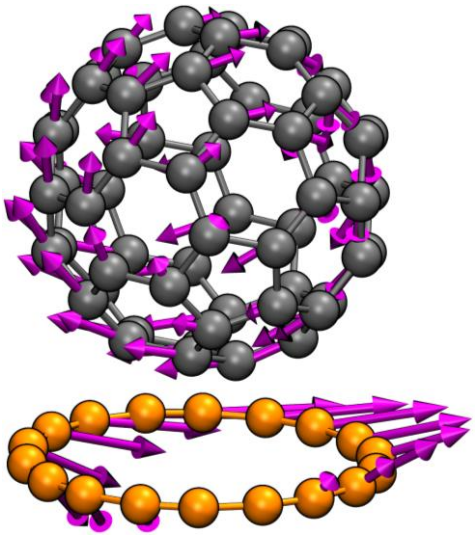

Fig. 4 Normal coordinate of the only imaginary frequency of the transition state linking two minimum configurations of the $C_{60}@C_{18}$ dimer.

After a C_{60} fullerene and a cyclocarbon form a dimer, another cyclocarbon or fullerene can be further combined with it to form a trimer. In the following two sections, we investigated the possible geometric structures, binding strength, and interaction nature of trimers composed of C_{60} fullerene and cyclocarbon with 1:2 and 2:1 manners.

3.2 Trimerization of one C_{60} fullerene with two cyclocarbons

This section considers the case of one C_{60} fullerene combined with two cyclocarbons to form $C_{60}@2C_n$ trimers, where n = 18, 22, 26, 30, and 34.

The optimized structures of the trimers composed of one C_{60} fullerene and two cyclocarbons are shown in Fig. 5. The IGMH δg^{inter} isosurfaces represented in blue and green reveal the main interaction regions between monomers, and the angle between the fitting planes of the two cyclocarbons is also shown. It can be seen that in all trimers, due to π-π interactions, the two cyclocarbons bind to each other and are always closely attached to the C_{60} fullerene. As the size of the cyclocarbons increases, the angle between the two rings decreases gradually, and at the same time, C_{60}

https://doi.org/10.26434/chemrxiv-2024-hs2sz **ORCID:** https://orcid.org/0000-0002-7079-1907 Content not peer-reviewed by ChemRxiv. **License:** CC BY 4.0

fullerene is more and more completely wrapped by the cyclocarbons. When the size of the cyclocarbon reaches C_{34}, the two rings become perfectly parallel to each other. In this case, as emphasized by the blue isosurface in Fig. 5(e), a clear circular π-π stacking region is formed between the two C_{34}, and the fullerene is embedded precisely at its center. Incidentally, in $2C_{34}@C_{60}$, the shorter C-C bond of one cyclocarbon faces the longer C-C bond of another one, as observed in our study of π-π stacked C_{18} dimer, and this phenomenon can be well explained by the electrostatic potential complementary rule.[24,60]

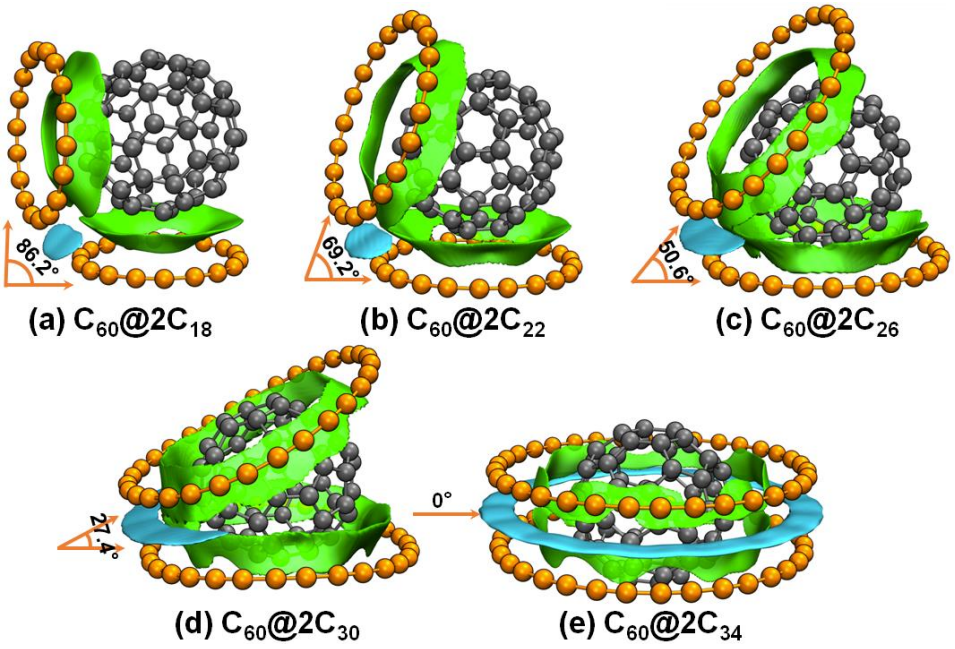

Fig. 5 Optimized geometry of $C_{60}@2C_n$ trimers (n = 18, 22, 26, 30, and 34). Isosurfaces of δg^{inter} function with isovalue of 0.003 a.u. are shown to reveal main interaction regions between two cyclocarbons (colored by blue) and between cyclocarbons and fullerene (colored by green). The angles between the fitting planes of the two cyclocarbons are also labelled.

Fig. 6(a) presents the binding energies for $C_{60}@C_n$ dimer formation between C_{60} fullerene and C_n (ΔE^1_{bind}) and for $C_{60}@2C_n$ trimer formation between $C_{60}@C_n$ and another C_n (ΔE^2_{bind}). Their sum ($\Delta E^{\text{tot}}_{\text{bind}}$) corresponds to the total binding energy between the three monomer molecules. It can be seen that $\Delta E^{\text{tot}}_{\text{bind}}$ becomes

https://doi.org/10.26434/chemrxiv-2024-hs2sz **ORCID:** https://orcid.org/0000-0002-7079-1907 Content not peer-reviewed by ChemRxiv. **License:** CC BY 4.0

increasingly negative as ring size increases, clearly indicating that the fullerene has a stronger tendency to aggregate into trimers with two relatively large-sized cyclocarbons. In addition, $\Delta E^{2}_{\text{bind}}$ is distinctly more negative than $\Delta E^{1}_{\text{bind}}$, denoting that the later added cyclocarbon bind more easily than the first one, and this trend is more pronounced for large-sized cyclocarbons. This phenomenon shows an evident synergistic effect brought by intermolecular interaction between cyclocarbons.

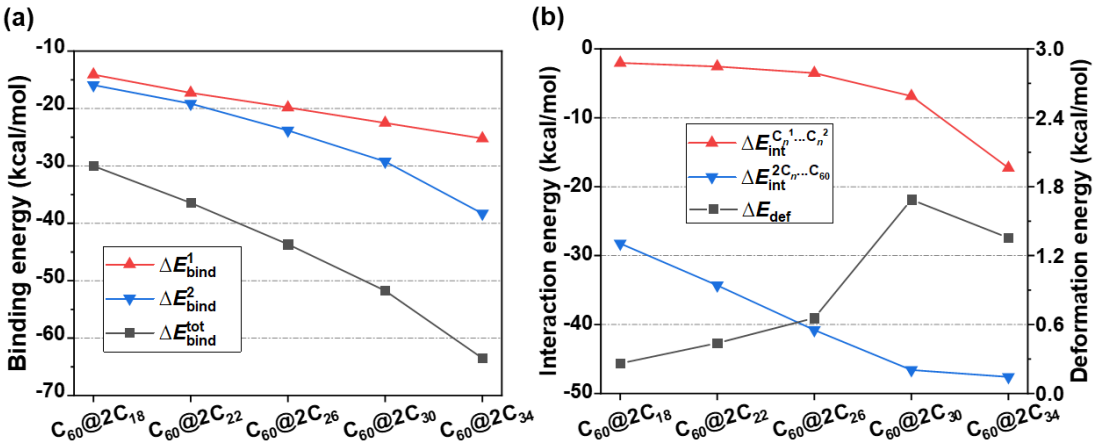

Fig. 6 (a) Binding energies for $C_{60}@C_n$ dimer formation between C_{60} fullerene and C_n ($\Delta E^{1}_{\text{bind}}$) and for $C_{60}@2C_n$ trimer formation between $C_{60}@C_n$ and another C_n ($\Delta E^{2}_{\text{bind}}$), as well as the total binding energy ($\Delta E^{\text{tot}}_{\text{bind}}$) of $2C_n@C_{60}$ trimers; (b) Interaction energy between two C_n ($\Delta E^{C_n^1 \cdots C_n^2}_{\text{int}}$) and between two C_n and C_{60} fullerene ($\Delta E^{2C_n \cdots C_{60}}_{\text{int}}$), as well as deformation energy of all molecules during complexation to trimer (ΔE_{def}).

We further characterized the interaction strength between the constituent monomers in the $C_{60}@2C_n$ trimer using interaction energy $\Delta E^{C_n^1 \cdots C_n^2}_{\text{int}} = E(2C_n) - [E(C_n^1) + E(C_n^2)]$ and $\Delta E^{2C_n \cdots C_{60}}_{\text{int}} = E(C_{60}@2C_n) - [E(C_{60}) + E(2C_n)]$, where $E(2C_n)$, $E(C_n^1)$, $E(C_n^2)$, $E(C_{60}@2C_n)$, and $E(C_{60})$ stand for the electronic energies calculated for the complex of two cyclocarbons, the first cyclocarbon, the second cyclocarbon, the $C_{60}@2C_n$ trimer, and the C_{60} fullerene, respectively. All energies were evaluated based

https://doi.org/10.26434/chemrxiv-2024-hs2sz **ORCID:** https://orcid.org/0000-0002-7079-1907 Content not peer-reviewed by ChemRxiv. **License:** CC BY 4.0

on optimized trimer geometries. It is found from the $\Delta E_{\text{int}}^{C_n^1 \cdots C_n^2}$ in Fig. 6(b) that the interaction strength between the two cyclocarbons increases steadily and slowly as the ring size varies from C_{18} to C_{30}. The interaction between the two C_{34} rings in $C_{60}@2C_{34}$ is quite significant (-17.3 kcal/mol), which is in line with the observation in Fig. 5 that only two C_{34} can form a complete π-π interaction with each other, while this interaction in other trimer can only occur within a very limited contact area.

As can be seen from $\Delta E_{\text{int}}^{2C_n \cdots C_{60}}$ in Fig. 6(b), the interaction strength between C_{60} fullerene and the two cyclocarbons increases linearly and rapidly with increasing ring size from C_{18} to C_{30}. However, the situation is different for the case of $C_{60}@2C_{34}$, as the interaction between two C_{34} and C_{60} fullerene is not much stronger than that in $C_{60}@2C_{30}$, mainly due to the large ring size of C_{34} preventing fullerene from perfectly interacting with the two stacked C_{34}, as shown in Fig. 1(d). This is also supported by the fact that the average width of the δg^{inter} isosurfaces between the cyclocarbons and fullerene in $2C_{34}@C_{60}$ is notably lower than that in other trimers.

Fig. 6(b) also shows the deformation energy (ΔE_{def}) of the studied trimer, which is inferred to be almost entirely contributed by two cyclocarbons, as fullerene has a very rigid framework. It can be seen that ΔE_{def} increases with ring size, mainly because the larger the carbon ring, the more flexible it is, and thus the easier it is to deform due to external influences. Once again, the $C_{34}@C_{60}$ shows its specificity because the two stacked C_{34} interact "incompletely" with C_{60} fullerene relative to other cyclocarbons, resulting in their being less affected.

3.3 Trimerization of two C_{60} fullerenes with one cyclocarbon

This section considers the case of two C_{60} fullerenes combined with one cyclocarbon to form $2C_{60}@C_n$ trimers, where n = 18, 22, 26, and 30.

The optimized structures of the trimers composed of two C_{60} fullerenes and a cyclocarbon are shown in Fig. 7. The IGMH δg^{inter} isosurfaces represented in yellow and green reveal the main interaction regions between monomers, and the minimum distance between the two fullerenes (d_{min}) is also shown in the graph. For complex

https://doi.org/10.26434/chemrxiv-2024-hs2sz **ORCID:** https://orcid.org/0000-0002-7079-1907 Content not peer-reviewed by ChemRxiv. **License:** CC BY 4.0

$2C_{60}@C_{18}$, it can be seen that there is an evident interaction between the C_{18} and C_{60} fullerenes, but the small size of the carbon ring hinders the close contact between fullerenes, resulting in a d_{min} of up to 4.86 Å, which is obviously much longer than the sum of the vdW radius of the two carbons (~ 3.40 Å). As the ring size increases to C_{22}, there is not only a significant $C_{60}…C_{22}$ interaction, but also an obvious interaction between two C_{60} fullerenes in the $2C_{60}@C_{22}$, as shown by the yellow isosurface and small d_{min}. With the complex comes to $2C_{60}@C_{26}$, although the $C_{60}…C_{60}$ interaction is further enhanced, as shown by the yellow isosurface becoming wider and d_{min} decreasing to 3.05 Å, the interaction between cyclocarbon and fullerene is weakened to a certain extent, which is vividly reflected by the narrowed green isosurface. Therefore, it is inferred that $2C_{60}@C_{26}$ and $2C_{60}@C_{22}$ may have comparable stability. Finally, in the case of $2C_{60}@C_{30}$, the oversized ring of C_{30} makes it difficult to symmetrically bind two C_{60} fullerenes. So, only one C_{60} fullerene interacts with all atoms on the cyclocarbon, while the other one binds obliquely to the cyclocarbon, resulting in a relatively limited interaction. Therefore, it is reasonable to expect that $2C_{60}@C_{30}$ is less stable than $2C_{60}@C_{22}$ and $2C_{60}@C_{26}$.

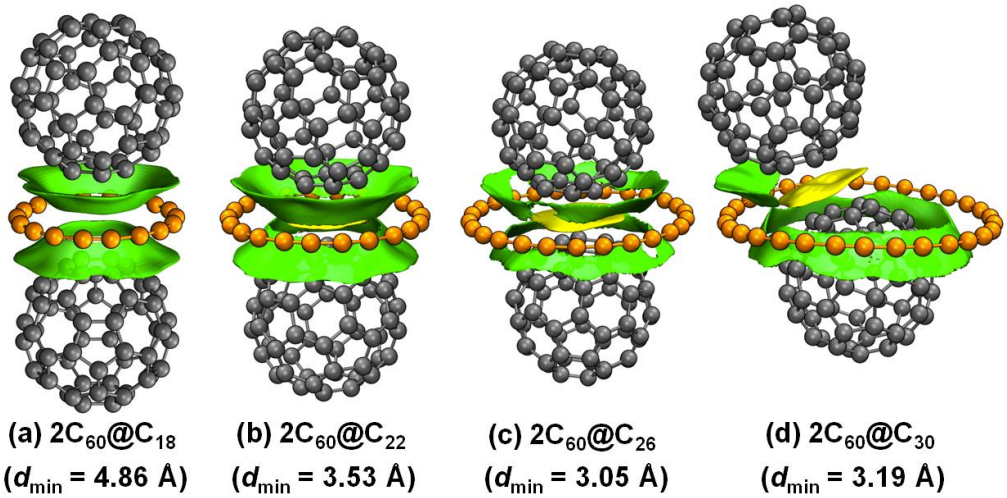

Fig. 7 Optimized geometry of $2C_{60}@C_n$ trimers (n = 18, 22, 26, and 30). Isosurfaces of δg^{inter} function with isovalue of 0.003 a.u. are shown to reveal main interaction regions between two fullerenes (colored by yellow) and between fullerene and cyclocarbons (colored by green). The minimum distances (d_{min}) between the two fullerenes are also shown.

https://doi.org/10.26434/chemrxiv-2024-hs2sz **ORCID:** https://orcid.org/0000-0002-7079-1907 Content not peer-reviewed by ChemRxiv. **License:** CC BY 4.0

Fig. 8(a) presents the binding energies for $C_{60}@C_n$ dimer formation between C_{60} fullerene and C_n (ΔE^1_{bind}) and for $2C_{60}@C_n$ trimer formation between $C_{60}@C_n$ and another C_{60} (ΔE^2_{bind}). It can be seen that for the complexes involving C_{18}, C_{22}, and C_{26}, the binding energy of the second C_{60} fullerene is clearly more negative than that of the first one, that is, the presence of the first C_{60} fullerene significantly promotes the binding of the second one, reflecting a synergistic effect within the systems. However, if the size of the cyclocarbon is too large to bind two C_{60} fullerenes compactly at the same time, not only will there be no synergistic effect, but anti-synergistic effect will occur. This is the case for $2C_{60}@C_{30}$. When the second C_{60} fullerene binds in $2C_{60}@C_{30}$, the energy reduction is only half that of the first one, which results in the total binding energy of $2C_{60}@C_{30}$ being more positive relative to that of $2C_{60}@C_{26}$. From the perspective of total binding energy, $2C_{60}@C_{22}$ and $2C_{60}@C_{26}$ have similar and most stable bond strengths, confirming our above inference by IGMH analysis, and it can be seen that C_{22} and C_{26} have the strongest ability to "glue" two C_{60} fullerenes together.

We further characterized the interaction strength between the constituent monomers in the $2C_{60}@C_n$ trimer using interaction energy $\Delta E_{\text{int}}^{C_{60}^1\cdots C_{60}^2} = E(2C_{60}) - [E(C_{60}^1) + E(C_{60}^2)]$ and $\Delta E_{\text{int}}^{2C_{60}\cdots C_n} = E(2C_{60}@C_n) - [E(2C_{60}) + E(C_n)]$, where $E(2C_{60})$, $E(C_{60}^1)$, $E(C_{60}^2)$, $E(2C_{60}@C_n)$, and $E(C_n)$ stand for the electronic energies calculated for the complex of two C_{60} fullerenes, the first C_{60} fullerene, the second C_{60} fullerene, the $2C_{60}@C_n$ trimer, and the cyclocarbon, respectively. All energies were evaluated based on optimized trimer geometries. It is found from the $\Delta E_{\text{int}}^{C_{60}^1\cdots C_{60}^2}$ in Fig. 8(b) that as the size of cyclocarbon increases, the interaction strength between the fullerenes slowly increases because the existence of the cyclocarbon hinders their close contact. From the interaction between two C_{60} fullerenes and cyclocarbon ($\Delta E_{\text{int}}^{2C_{60}\cdots C_n}$), it can

https://doi.org/10.26434/chemrxiv-2024-hs2sz **ORCID:** https://orcid.org/0000-0002-7079-1907 Content not peer-reviewed by ChemRxiv. **License:** CC BY 4.0

be seen that the medium-sized C_{22} and C_{26} interact most strongly with fullerenes, the C_{18} interacts weakly due to its smaller number of atoms, and the C_{30} interacts less strongly due to its loose binding with one of the fullerenes. The deformation energy in Fig. 8(b) indicates that the larger the carbon ring, the more likely it is to increase the system energy due to structural change during formation of the $2C_{60}@C_n$ trimer. But even for $2C_{60}@C_{30}$ with the maximum deformation energy, this value is only about 1.0 kcal/mol, which creates negligible hindrance to the complexation.

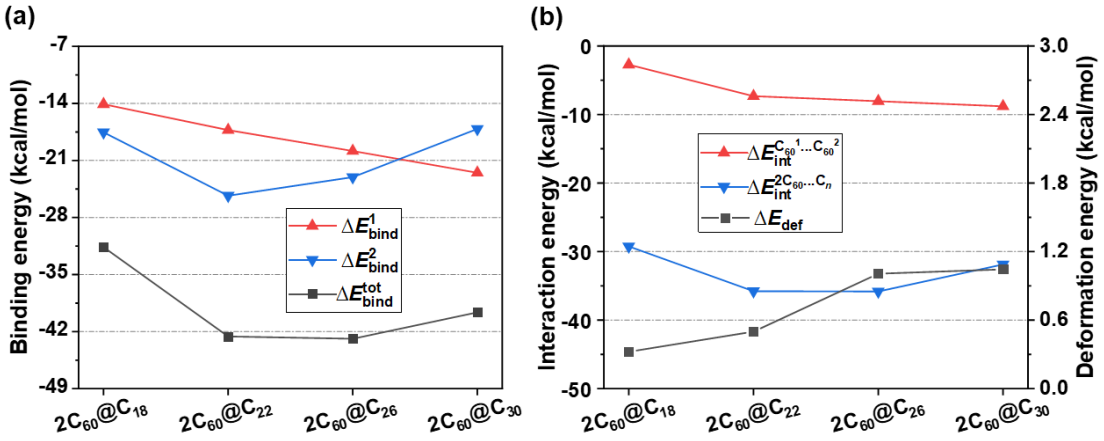

Fig. 8 (a) Binding energies for $C_{60}@C_n$ dimer formation between C_{60} fullerene and C_n (ΔE^1_{bind}) and for $2C_{60}@C_n$ trimer formation between $C_{60}@C_n$ and another C_{60} (ΔE^2_{bind}), as well as the total binding energy (ΔE^{tot}_{bind}) of $2C_{60}@C_n$ trimers; (b) Interaction energy between two C_{60} fullerenes ($\Delta E_{int}^{C_{60}^1 \cdots C_{60}^2}$) and between two C_{60} fullerenes and C_n ($\Delta E_{int}^{2C_{60} \cdots C_n}$), as well as deformation energy of all molecules during complexation to trimer (ΔE_{def}).

The vdW potential proposed by one of us is a particularly useful method for intuitively understanding vdW interaction between a molecule of interest and surrounding molecules.[61] Here, we use the vdW potential based on the Lennard-Jones parameters of Generation Amber Force Field (GAFF) forcefield[62] to delve into how the cyclocarbon acts as a "glue" to aid in the binding of two C_{60} fullerenes. Carbon is used as the probe atom, and complexes $2C_{60}@C_{22}$ and $2C_{60}@C_{30}$ are taken as examples. The vdW potentials generated by the cyclocarbon in these two

https://doi.org/10.26434/chemrxiv-2024-hs2sz **ORCID:** https://orcid.org/0000-0002-7079-1907 Content not peer-reviewed by ChemRxiv. **License:** CC BY 4.0

systems are plotted as isosurface maps and colored section maps in Fig. 9. In Fig. 9(a), the atoms in fullerenes are colored according to the vdW potential—the bluer the color, the more negative the vdW potential, and the stronger the dispersion attraction from the cyclocarbon felt by the corresponding fullerene atoms. From the maps of $2C_{60}@C_{22}$, it can be intuitively seen that the region where the vdW potential generated by C_{22} is obviously negative, that is, the region where the dispersion attraction interaction greatly exceeds the exchange-repulsion effect, mainly covers the axial area near the center of C_{22} with slight outward extension at both ends. This region simultaneously covers more than one-third of atoms in the two C_{60} fullerenes. Obviously, due to the distribution characteristics of the vdW potential caused by the unique structure of the C_{22}, this cyclocarbon can significantly promote the complexation between two fullerenes. In sharp contrast to the case of $2C_{60}@C_{22}$, in $2C_{60}@C_{30}$, the region with a significantly negative vdW potential of C_{30} covers nearly half of the atoms of one C_{60} fullerene, while for another fullerene, only a small portion can be covered. This is the main reason why the ΔE^2_{bind} of $2C_{60}@C_{30}$ is obviously more positive than the ΔE^1_{bind}. But even so, since ΔE^2_{bind} (-17.1 kcal/mol) is more than twice the energy of C_{60} fullerene dimerization (-8.3 kcal/mol, as mentioned earlier), the presence of C_{30} is significantly helpful in promoting fullerene dimerization.

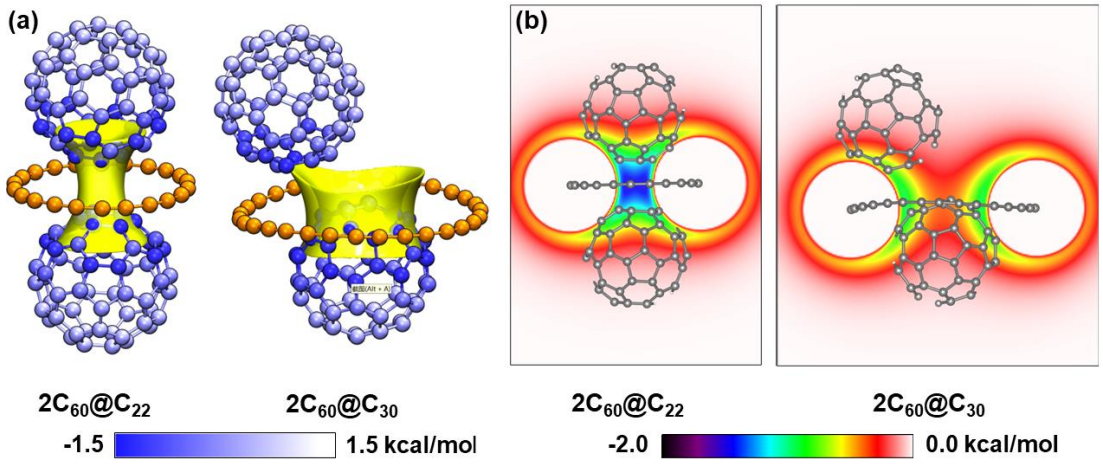

Fig. 9 VdW potential generated by the cyclocarbon in $2C_{60}@C_{22}$ and $2C_{60}@C_{30}$ with carbon as

https://doi.org/10.26434/chemrxiv-2024-hs2sz **ORCID:** https://orcid.org/0000-0002-7079-1907 Content not peer-reviewed by ChemRxiv. **License:** CC BY 4.0

the probe atom: (a) Isosurface map with isovalue of -0.8 kcal/mol, atoms are colored by vdW potential according to the color bar; (b) Section maps colored according to the color bar.

4. Summary

In this work, for the first time, we conducted in-depth theoretical studies on the non-covalent complexes formed by cyclocarbons of different sizes and the most representative C_{60} fullerene, in order to reveal the structure, binding strength, and interaction nature of them. By means of high-precision density functional calculations, we found that the binding energy between cyclocarbons and C_{60} fullerenes is more than -14.4 kcal/mol, which is much stronger than that of C_{18} dimer and C_{60} fullerene dimer, suggesting the particularly strong affinity between cyclocarbon and fullerene. According to binding free energy, the combination of cyclocarbons and C_{60} fullerene in the gas phase is found to be spontaneous at room temperature, and the hydrophobic effect arising from solvent environment can facilitate their binding. Until C_{34}, the binding strength of the cyclocarbons with C_{60} fullerene increases almost linearly with the increasing size, and the dimer of C_{34} and fullerene forms a perfect nano-Saturn structure. However, cyclocarbons larger than C_{34} have a reduced interaction with fullerene, because not all of their atoms can contact fullerenes closely. IGMH map, sobEDAw energy decomposition, fragment charges, and intermolecular total Mayer bond order collectively confirmed that the dimerization between cyclocarbon and fullerene is driven by the π-π stacking effect. The relative rotation between the monomers is found to be extremely easy due to negligible barrier.

We examined the trimers formed by cyclocarbons and C_{60} fullerene in a 2:1 ratio, namely $2C_n@C_{60}$ (n = 18, 22, 26, 30, and 34). As the ring size increases, the angle between the two cyclocarbons gradually decreases. In the largest trimer we studied, $2C_{34}@C_{60}$, the fullerene is symmetrically surrounded by two cyclocarbons, and the trimerization energy is as high as -64.9 kcal/mol. The molecular interactions between the trimers are carefully discussed by analyzing interaction energies and the very intuitive IGMH isosurface maps. By studying the trimers in the form of 1:2 between

https://doi.org/10.26434/chemrxiv-2024-hs2sz **ORCID:** https://orcid.org/0000-0002-7079-1907 Content not peer-reviewed by ChemRxiv. **License:** CC BY 4.0

cyclocarbon and fullerenes, that is $2C_{60}@C_n$ (n = 18, 22, 26, and 30), it is observed that when the size of the cyclocarbon sandwiched between two fullerenes is not very large, the trimer exhibits an ideal dumbbell-like structure, and the presence of the first fullerene has a significant synergistic effect on the binding of the second one. On the contrary, larger cyclocarbons like C_{34} have an anti-cooperative effect. Combined with the analysis of interaction energy and vdW potential, we point out that the existence of cyclocarbon can greatly promote the non-covalent dimerization of fullerenes; in other words, the cyclocarbon acts as a "molecular glue".

This work will help chemists gain insight into the non-covalent aggregation between cyclocarbons and fullerenes, so as to design supramolecular systems composed of them or their analogues. The conclusions of this article also have reference significance for exploring the complexation between other types of cyclic molecules and spherical molecules or atomic clusters. In the following work, we plan to further explore the self-assembly behavior of cyclocarbons and fullerenes in the gas phase and condensed phase through molecular simulations to further understand the dynamic process of their interaction.

Supplemental information

xyz files of all studied complexes involved in this work, optimized geometry of two configurations of $C_{60}@C_{18}$ dimer, deformation energy and binding energies (kcal/mol) of $C_{60}@C_n$ (n = 18, 20, 22, 24, 26, 28, 30, 32, 34, and 36) dimers, relationship between area of IGMH δg^{inter} isosurface of 0.002 a.u. and binding energy of $C_{60}@C_n$ (n = 18, 20, 22, 24, 26, 28, 30, 32, and 34), conformational superpositions of C_{36} in isolated state and after complexation with fullerene.

Conflicts of interest

The authors declare no conflict of interest.

https://doi.org/10.26434/chemrxiv-2024-hs2sz **ORCID:** https://orcid.org/0000-0002-7079-1907 Content not peer-reviewed by ChemRxiv. **License:** CC BY 4.0

References

[1] F. Diederich, Y. Rubin, C. B. Knobler, R. L. Whetten, et al., All-carbon molecules: Evidence for the generation of cyclo[18]carbon from a stable organic precursor. *Science* **1989**, *245*, 1088.

[2] F. Diederich, M. Kivala, All-carbon scaffolds by rational design. *Adv. Mater.* **2010**, *22*, 803.

[3] S. W. McElvany, M. M. Ross, N. S. Goroff, F. Diederich, Cyclocarbon coalescence: Mechanisms for tailor-made fullerene formation. *Science* **259**, 1594.

[4] G. von Helden, N. G. Gotts, M. T. Bowers, Experimental evidence for the formation of fullerenes by collisional heating of carbon rings in the gas phase. *Nature* **1993**, *363*, 60.

[5] K. Kaiser, L. M. Scriven, F. Schulz, P. Gawel, et al., An sp-hybridized molecular carbon allotrope, cyclo[18]carbon. *Science* **2019**, *365*, 1299.

[6] W. Xu, L. Sun, W. Zheng, W. Gao, et al., On-surface synthesis of anti-aromatic cyclo[12]carbon and aromatic cyclo[6]carbon. *ResearchSquare* **2023**, DOI: 10.21203/rs.3.rs-3411973/v1.

[7] L. Sun, W. Zheng, W. Gao, F. Kang, et al., On-surface synthesis of aromatic cyclo[10]carbon and cyclo[14]carbon. *Nature* **2023**, *623*, 972.

[8] F. Albrecht, I. Rončević, Y. Gao, F. Paschke, et al., The odd-number cyclo[13]carbon and its dimer cyclo[26]carbon. *ChemRxiv* **2024**, DOI: 10.26434/chemrxiv-2023-ddrh7-v2.

[9] Y. Gao, F. Albrecht, I. Rončević, I. Ettedgui, et al., On-surface synthesis of a doubly anti-aromatic carbon allotrope. *Nature* **2023**, *623*, 977.

[10] W. Xu, L. Sun, W. Zheng, F. Kang, On-surface synthesis and characterization of anti-aromatic cyclo[20]carbon. *ResearchSquare* **2023**, DOI: 10.21203/rs.3.rs-3411934/v1.

[11] Y. Wu, X. Yan, Z. Liu, T. Lu, Double aromaticity of Franck-Condon excited states of Cyclo[16]carbon. *ChemRxiv* **2023**, DOI: 10.26434/chemrxiv-2023-mtx00.

[12] Y. Wu, Z. Liu, T. Lu, M. Orozco-Ic, et al., Exploring the aromaticity differences of isoelectronic species of cyclo[18]carbon (C_{18}), $B_6C_6N_6$, and B_9N_9: The role of carbon atoms as connecting bridges. *Inorg. Chem.* **2023**, *62*, 19986.

[13] X. Wang, Z. Liu, J. Wang, T. Lu, et al., Electronic structure and aromaticity of an unusual cyclo[18]carbon precursor, $C_{18}Br_6$. *Chem.-Eur. J.* **2023**, *29*, e202300348.

[14] Z. Liu, X. Wang, T. Lu, X. Yan, et al., Theoretical design of a dual-motor nanorotator composed of all-carboatomic cyclo[18]carbon and a figure-of-eight carbon hoop. *Chem. Commun.* **2023**, *59*, 9770.

[15] Z. Liu, X. Wang, T. Lu, J. Wang, et al., Molecular assembly with a figure-of-eight nanohoop as a strategy for the collection and stabilization of cyclo[18]carbon. *Phys. Chem. Chem. Phys.* **2023**, *25*, 16707.

[16] X. Wang, Z. Liu, X. Yan, T. Lu, et al., Bonding character, electron delocalization, and aromaticity of cyclo[18]carbon (C_{18}) precursors, C_{18}-$(CO)_n$ (n = 6, 4, and 2): Focusing on the effect of carbonyl (-CO) Groups. *Chem.-Eur. J.* **2022**, *28*, e202103815.

[17] X. Wang, Z. Liu, X. Yan, T. Lu, et al., Photophysical properties and optical nonlinearity of cyclo[18]carbon (C_{18}) precursors, C_{18}-$(CO)_n$ (n = 2, 4, and 6): Focusing on the effect of the carbonyl groups. *Phys. Chem. Chem. Phys.* **2022**, *24*, 7466.

[18] T. Lu, Z. Liu, Q. Chen, Accurate theoretical evaluation of strain energy of all-carboatomic ring (cyclo[2*n*]carbon), boron nitride ring, and cyclic polyacetylene. *Chinese Phys. B* **2022**, *31*, 126101.

[19] Z. Liu, X. Wang, T. Lu, A. Yuan, et al., Potential optical molecular switch: Lithium@cyclo[18]carbon complex transforming between two stable configurations. *Carbon* **2022**, *187*, 78.

https://doi.org/10.26434/chemrxiv-2024-hs2sz **ORCID:** https://orcid.org/0000-0002-7079-1907 Content not peer-reviewed by ChemRxiv. **License:** CC BY 4.0

[20] T. Lu, Z. Liu, Q. Chen, Comment on "18 and 12 – member carbon rings (cyclo[*n*]carbons) – A density functional study". *Mat. Sci. Eng. B* **2021**, *273*, 115425.
[21] T. Lu, Q. Chen, Ultrastrong regulation effect of the electric field on the all-carboatomic ring cyclo[18]carbon. *ChemPhysChem* **2021**, *22*, 386.
[22] Z. Liu, T. Lu, A. Yuan, X. Wang, et al., Remarkable size effect on photophysical and nonlinear optical properties of all-carboatomic rings, cyclo[18]carbon and its analogues. *Chem.-Asian J.* **2021**, *16*, 2267.
[23] Z. Liu, T. Lu, Q. Chen, Comment on "Theoretical investigation on bond and spectrum of cyclo[18]carbon (C_{18}) with sp-hybridized". *J. Mol. Model.* **2021**, *27*, 42.
[24] Z. Liu, T. Lu, Q. Chen, Intermolecular interaction characteristics of the all-carboatomic ring, cyclo[18]carbon: Focusing on molecular adsorption and stacking. *Carbon* **2021**, *171*, 514.
[25] Z. Liu, T. Lu, Q. Chen, Vibrational spectra and molecular vibrational behaviors of all-carboatomic rings, cyclo[18]carbon and its analogues. *Chem. – Asian J.* **2021**, *16*, 56.
[26] Z. Liu, T. Lu, Q. Chen, An sp-hybridized all-carboatomic ring, cyclo[18]carbon: Electronic structure, electronic spectrum, and optical nonlinearity. *Carbon* **2020**, *165*, 461.
[27] Z. Liu, T. Lu, Q. Chen, An sp-hybridized all-carboatomic ring, cyclo[18]carbon: Bonding character, electron delocalization, and aromaticity. *Carbon* **2020**, *165*, 468.
[28] S. Schrettl, C. Stefaniu, C. Schwieger, G. Pasche, et al., Functional carbon nanosheets prepared from hexayne amphiphile monolayers at room temperature. *Nat. Chem.* **2014**, *6*, 468.
[29] G. von Helden, N. Gotts, M. T. Bowers. Experimental evidence for the formation of fullerenes by collisional heating of carbon rings in the gas phase. *Nature* **1993**, *363*, 60.
[30] K. S. Novoselov, A. K. Geim, S. V. Morozov, D. Jiang, et al., Electric field effect in atomically thin carbon films. *Science* **2004**, *306*, 666.
[31] H. W. Kroto, J. R. Heath, S. C. O'Brien, R. F. Curl, et al., C_{60}: Buckminsterfullerene. *Nature* **1985**, *318*, 162.
[32] J. L. Chen, R. Q. Zhang, Strong interaction between cyclo[18]carbon and graphene. *Adv. Theor. Simul.* **2021**, *4*, 2100022.
[33] J.-D. Chai, M. Head-Gordon, Long-range corrected hybrid density functionals with damped atom-atom dispersion corrections. *Phys. Chem. Chem. Phys.* **2008**, *10*, 6615.
[34] M. J. Frisch, J. A. Pople, J. S. Binkley, Self-consistent molecular orbital methods 25. Supplementary functions for Gaussian basis sets. *J. Chem. Phys.* **1984**, *80*, 3265.
[35] M. J. Frisch, G. W. Trucks, H. B. Schlegel, G. E. Scuseria, et al., Gaussian 16 A.03. Wallingford, CT, **2016**.
[36] N. Mardirossian, M. Head-Gordon, ωB97M-V: A combinatorially optimized, range-separated hybrid, meta-GGA density functional with VV10 nonlocal correlation. *J. Chem. Phys.* **2016**, *144*, 214110.
[37] F. Weigend, R. Ahlrichs, Balanced basis sets of split valence, triple zeta valence and quadruple zeta valence quality for H to Rn: Design and assessment of accuracy. *Phys. Chem. Chem. Phys.* **2005**, *7*, 3297.
[38] F. Neese, F. Wennmohs, U. Becker, C. Riplinger, The ORCA quantum chemistry program package. *J. Chem. Phys.* **2020**, *152*, 224108.
[39] S. Grimme, J. Antony, S. Ehrlich, H. Krieg, A consistent and accurate ab initio parametrization of density functional dispersion correction (DFT-D) for the 94 elements H-Pu. *J. Chem. Phys.* **2010**, *132*, 154104.

https://doi.org/10.26434/chemrxiv-2024-hs2sz **ORCID:** https://orcid.org/0000-0002-7079-1907 Content not peer-reviewed by ChemRxiv. **License:** CC BY 4.0

[40] H. Kruse, S. Grimme, A geometrical correction for the inter- and intra-molecular basis set superposition error in Hartree-Fock and density functional theory calculations for large systems. *J. Chem. Phys.* **2012**, *136*, 154101.
[41] T. Lu, Q. Chen, Shermo: A general code for calculating molecular thermochemistry properties. *Comput. Theor. Chem.* **2021**, *1200*, 113249.
[42] S. Grimme, Supramolecular binding thermodynamics by dispersion-corrected density functional theory. *Chem.-Eur. J.* **2012**, *18*, 9955.
[43] A. V. Marenich, C. J. Cramer, D. G. Truhlar, Universal solvation model based on solute electron density and on a continuum model of the solvent defined by the bulk dielectric constant and atomic surface tensions. *J. Phys. Chem. B* **2009**, *113*, 6378.
[44] C. P. Kelly, C. J. Cramer, D. G. Truhlar, Aqueous solvation free energies of ions and ion-water clusters based on an accurate value for the absolute aqueous solvation free energy of the proton. *J. Phys. Chem. B* **2006**, *110*, 16066.
[45] T. Lu, Q. Chen, Simple, efficient, and universal energy decomposition analysis method based on dispersion-corrected density functional theory. *J. Phys. Chem. A* **2023**, *127*, 7023.
[46] T. Lu, F. Chen, Multiwfn: A multifunctional wavefunction analyzer. *J. Comput. Chem.* **2012**, *33*, 580.
[47] T. Lu, Q. Chen, Independent gradient model based on Hirshfeld partition: A new method for visual study of interactions in chemical systems. *J. Comput. Chem.* **2022**, *43*, 539.
[48] T. Lu, Q. Chen, Visualization analysis of weak interactions in chemical systems. In Comprehensive Computational Chemistry 2, Elsevier, **2023**, p. 240.
[49] W. Humphrey, A. Dalke, K. Schulten, VMD: visual molecular dynamics. *J. Mol. Graph.* **1996**, *14*, 33.
[50] K. Momma, F. Izumi, VESTA 3 for three-dimensional visualization of crystal, volumetric and morphology data. *J. Appl. Crystallogr.* **2011**, *44*, 1272.
[51] S. M. Bachrach, Planar rings in nano-Saturns and related complexes. *Chem. Commun.* **2019**, *55*, 3650.
[52] D. I. Sharapa, J. T. Margraf, A. Hesselmann, T. Clark, Accurate intermolecular potential for the C_{60} dimer: The performance of different levels of quantum theory. *J. Chem. Theory Comput.* **2017**, *13*, 274.
[53] A. D. Becke, A new mixing of hartree-fock and local density-functional theories. *J. Chem. Phys.* **1993**, *98*, 1372.
[54] L. Goerigk, A. Hansen, C. Bauer, S. Ehrlich, et al., A look at the density functional theory zoo with the advanced GMTKN55 database for general main group thermochemistry, kinetics and noncovalent interactions. *Phys. Chem. Chem. Phys.* **2017**, *19*, 32184.
[55] S. Grimme, Do special noncovalent π–π stacking interactions really exist? *Angew. Chem. Int. Ed.* **2008**, *47*, 3430.
[56] T. Lu, F. Chen, Comparison of computational methods for atomic charges. *Acta Phys. -Chim. Sin.* **2012**, *28*, 1.
[57] R. S. Mulliken, Electronic population analysis on LCAO-MO molecular wave functions. II. Overlap populations, bond orders, and covalent bond energies. *J. Chem. Phys.* **1955**, *23*, 1841.
[58] T. Lu, F. Chen, Atomic dipole moment corrected hirshfeld population method. *J. Theor. Comp. Chem.* **2012**, *11*, 163.
[59] I. Mayer, Charge, bond order and valence in the ab initio SCF theory. *Chem. Phys. Lett.* **1983**, *97*, 270.

https://doi.org/10.26434/chemrxiv-2024-hs2sz **ORCID:** https://orcid.org/0000-0002-7079-1907 Content not peer-reviewed by ChemRxiv. **License:** CC BY 4.0

[60] T. Lu, F. Chen, Revealing the nature of intermolecular interaction and configurational preference of the nonpolar molecular dimers $(H_2)_2$, $(N_2)_2$, and $(H_2)(N_2)$. *J. Mol. Model.* **2013**, *19*, 5387.
[61] T. Lu, Q. Chen, van der Waals potential: an important complement to molecular electrostatic potential in studying intermolecular interactions. *J. Mol. Model.* **2020**, *26*, 315.
[62] J. Wang, R. M. Wolf, J. W. Caldwell, P. A. Kollman, et al., Development and testing of a general amber force field. *J. Comput. Chem.* **2004**, *25*, 1157.

https://doi.org/10.26434/chemrxiv-2024-hs2sz **ORCID:** https://orcid.org/0000-0002-7079-1907 Content not peer-reviewed by ChemRxiv. **License:** CC BY 4.0